Higher-Dimensional Caustics in Nonlinear Compton Scattering

Vasily Yu. Kharin,[1,*] Daniel Seipt,[2,3,†] and Sergey G. Rykovanov[1,‡]

[1]*Helmholtz-Institut Jena, Fröbelstieg 3, 07743 Jena, Germany*
[2]*Lancaster University, Physics Department, Bailrigg, Lancaster LA1 4YW, United Kingdom*
[3]*Cockcroft Institute, Daresbury Laboratory, Keckwick Ln, Warrington WA4 4AD, United Kingdom*

A description of the spectral and angular distributions of Compton scattered light in collisions of intense laser pulses with high-energy electrons is unwieldy and usually requires numerical simulations. However, due to the large number of parameters affecting the spectra such numerical investigations can become computationally expensive. Using methods of catastrophe theory we predict higher-dimensional caustics in the spectra of the Compton scattered light, which are associated with bright narrow-band spectral lines, and in the simplest case can be controlled by the value of the linear chirp of the pulse. These findings require no full-scale calculations and have direct consequences for the photon yield enhancement of future nonlinear Compton scattering x-ray or gamma-ray sources.

The ongoing interest in a precise theoretical description of nonlinear Compton scattering—the scattering of intense laser light off an electron beam—is nowadays driven by the prospects of using it as a source of collimated, ultrafast, tunable, bright, and narrow-band x rays and gamma rays [1–8]. While the basic mechanism for the hard photon production is a Doppler up-shift of the laser frequency, an accurate description of the backscattered spectrum, and hence the source's properties, requires us to take into account, apart from the electron beam properties, also the laser pulse intensity, shape, and potential frequency modulation (chirp). Because the number of scattered photons is proportional to $a_0^2 = 0.73 I_{18} \lambda_{\mu m}^2$, where I_{18} is the peak laser pulse intensity in units of 10^{18} W/cm^2 and $\lambda_{\mu m}$ is the central wavelength in microns, the laser pulse intensity should be as large as possible to maximize the photon yield. However, the interaction becomes nonlinear when $a_0 \gtrsim 1$. Apart from the up-shifting of the scattered radiation frequency, there is also an intensity-dependent redshift, which is, in the classical picture, caused by the longitudinal drift due to the $\mathbf{v} \times \mathbf{B}$ force [9–11]. This "slows" the electron down relative to its initial velocity. While in the case of a monochromatic plane wave the drift is uniform and the redshift is constant, the presence of an envelope of the laser pulse implies a time dependence of the Doppler shift. Hence, the so-called ponderomotive broadening of the spectral lines appears, preventing a narrow bandwidth and posing a severe limitation on the brightness of high-intensity Compton sources [12–15].

In order to operate narrow-band Compton sources one either has to limit the allowed laser intensity [9,16], or employ more advanced schemes with a frequency modulated (chirped) laser pulse. In the latter approaches a time-dependent frequency blueshift of the laser light mitigates the ponderomotive redshift [12]. In Refs. [13–15] an optimal chirping prescription has been derived by thoroughly analyzing theoretically the nonlinear Compton spectrum with chirped laser pulses. For optimal chirping the ponderomotive broadening is compensated completely, allowing narrow-band Compton sources even in the nonlinear regime $a_0 \gtrsim 1$. Unfortunately, the optimal chirp is a complicated nonlinear function of the laser phase, which might be hard to realize experimentally.

For practical purposes it is therefore important to investigate chirping schemes that are not perfectly optimal, but still significantly reduce the source bandwidth and increase its brightness. The problem is that every particular combination of envelope and frequency profiles of the laser pulse requires separate calculations. As a result, the question of the interrelation between the properties of the incident pulse and the frequency-angular distribution of the scattered radiation is very complicated. Only a very limited amount of closed form analytical solutions exist for finite laser pulses [10,11,17], typically employing the stationary phase method. This is the reason why expensive numerical investigations [18] and parameter surveys are typically required in order to find promising combinations of pulse shape and frequency modulation.

In this Letter, the theory of singularities of differentiable projection maps—also called catastrophe theory—is applied to the stationary phase picture, turning it into a powerful tool for theoretical investigations of the nonlinear Compton spectra. It is known from diffractive optics that the singularities, or caustics, are inherently related to the focusing of light, with a universal diffraction pattern near the caustics [19]. In our case spectral intensity can be focused causing narrow spectral peaks in the vicinity of spectral caustics [20,21]. We use this approach here to

identify higher-dimensional caustics that are used to predict bright and narrow spectral peaks. We investigate in detail the case of a linearly chirped laser pulse and find pairs of cusp caustics connected by two folds. Their disappearance with increasing chirp provides a so-called lips caustic [19,22,23]. The cusps evoke bright and narrow-band peaks in the spectrum that can be tuned by adjusting the linear chirp of the laser pulse. Thus, the investigation of spectral caustics can serve as a useful technique applicable to the design of the optimization schemes for Compton scattering x-ray and gamma-ray sources, guiding and complementing full-scale numerical simulations. Throughout the Letter we use units with $\hbar = c = 1$ and dimensionless spacetime ($x\omega_{L,0} \to x$) and energy ($\omega/\omega_{L,0} \to \omega$) variables by rescaling with the central laser frequency $\omega_{L,0}$.

The fundamental theoretical investigation of nonlinear Compton scattering started with the seminal works of Nikishov and Ritus back in the 1960s [24,25] with pulse shape effects included later on [26–30]. We shall briefly recall it here: nonlinear Compton scattering is described as a first-order strong-field QED process in the Furry picture. A photon is emitted by an electron dressed by a plane wave background laser field with vector potential $\mathbf{A}$, which is made dimensionless by the rescaling $e\mathbf{A}/m \to \mathbf{A}$. Here, e and m are the electron absolute charge and mass, respectively. In the Furry picture, the laser-dressed electrons are described as Volkov spinor wave functions $\Psi_{p,\sigma}$ [31], which are solutions of the Dirac equation with asymptotic four-momentum p and spin polarization σ.

The corresponding S-matrix element is given by

$$S_1 = -ie \int \bar{\Psi}_{q,\sigma'}(x) \varepsilon^* e^{i\kappa \cdot x} \Psi_{p,\sigma}(x) d^4 x. \tag{1}$$

Here, ε is the polarization vector of the scattered photon; $\kappa = (\omega, \boldsymbol{\kappa})$ is its four-wave vector. To simplify the expressions we consider the frame of reference where the electron is initially at rest, $p = (m, 0, 0, 0)$; we will refer to it as the electron frame, in contrast to the lab frame, where the electron is initially counterpropagating the laser pulse with energy γm. The laser pulse is propagating in the z direction and its vector potential depends only on the light-front time $\phi = t - z$. We therefore also introduce the light-front component of the scattered photon momentum $\kappa^- = \omega - \kappa^3$. The notation $\boldsymbol{\kappa}_\perp$ refers to the projection of the three-vector $\boldsymbol{\kappa}$ on the (x, y) plane.

By squaring the S matrix, averaging over the initial electron spin states, and summing over the polarizations of outgoing photon and electron, the differential photon emission probability is given by [17]

$$\frac{dW}{d\omega d\Omega} = \frac{e^2 \omega}{64\pi^3 m(m - \kappa^-)} \frac{1}{2} \sum_{\varepsilon\sigma\sigma'} |M_{\varepsilon\sigma'\sigma}|^2. \tag{2}$$

For a slowly varying laser pulse envelope the transition amplitude $M_{\varepsilon\sigma'\sigma}$ can be represented as a sum over harmonics by using a generalized Jacobi-Anger expansion [32],

$$M_{\varepsilon\sigma'\sigma} = \sum_{n=-\infty}^{+\infty} \int_{-\infty}^{+\infty} B_{\varepsilon\sigma'\sigma}^n(\phi)$$

$$\times \exp\left(i \int_0^\phi \frac{\omega + \kappa^- \mathbf{a}(\xi)^2/4}{1 - \frac{\kappa^-}{m}} - n\omega_L(\xi) d\xi \right) d\phi, \tag{3}$$

which is the basis for all further analysis. Here, the laser pulse is parametrized as $\mathbf{A} = (a_x(\phi)\cos\chi_L, a_y(\phi)\sin\chi_L, 0)$ with instantaneous frequency $\omega_L(\phi)$, phase $\chi_L(\phi) = \int_0^\phi \omega_L(\xi)d\xi$, and envelope $\mathbf{a}(\phi) = (a_x(\phi), a_y(\phi), 0)$ with the possibility for a time-dependent ellipticity [35].

Because the amplitudes for each harmonic $B_{\varepsilon\sigma'\sigma}^n(\phi)$ are slowly varying functions of ϕ [32], the value of the integrals in Eq. (3) can be estimated using the stationary phase approximation. Since the azimuthal direction of the emitted photon only affects the prefactors $B_{\varepsilon\sigma\sigma'}^n$, for the stationary phase analysis we can restrict ourselves to considering only one component of $\boldsymbol{\kappa}_\perp$, say, κ_x, assuming $\kappa_y = 0$. The stationary phase condition defines the so-called ray surfaces for the nth harmonic in the $(\kappa_x, \kappa_z, \phi)$ space:

$$F(\kappa_x, \kappa_z, \phi) = \sqrt{\kappa_x^2 + \kappa_z^2} \left[1 + \left(\frac{\mathbf{a}^2(\phi)}{4} + \frac{n\omega_L(\phi)}{m} \right) \right]$$

$$- \kappa_z \left(\frac{\mathbf{a}^2(\phi)}{4} + \frac{n\omega_L(\phi)}{m} \right) - n\omega_L(\phi) = 0 \tag{4}$$

with n being an integer number. For a fixed value of ϕ Eq. (4) defines a set of ellipses in the (κ_z, κ_x) plane for each harmonic, the size and eccentricity of which change continuously with ϕ.

The projection of the ray surface F on the (κ_x, κ_z) plane [Fig. 1(b)] defines the region of frequencies and angles where the scattered radiation will not be suppressed by rapid oscillations in the integrals in Eq. (3). This situation is similar to the one known in the catastrophe optics. The values of κ_x and κ_z play the role of control parameters, and the underlying integrals can be evaluated using the procedures similar to calculating diffraction patterns. The regular points of the projection map, where $\partial F/\partial \phi \neq 0$, contribute to the spectrum with the amplitudes defined by the stationary phase approximation. In contrast to that, the singular points of the map, where $\partial F/\partial \phi = 0$, are projected on the caustic set, and their contributions require higher-order corrections to evaluate the integrals in Eq. (3).

According to Thom's classification [36], there are only two types of stable singularities in systems with two control parameters. These are folds and cusps, see Fig. 2. In the vicinity of fold caustics the evaluation of the integrals in Eq. (3) yields Airy functions, while the cusp caustic (where also the second derivative of the ray surface vanishes) corresponds to the Pearcey integral [37]. In order to trace how these different caustics govern the Compton spectra let us consider two examples: a quasimonochromatic laser pulse and a linearly chirped pulse, both with circular polarization, i.e., $a_x = a_y$.

(a)

(b)

(c)
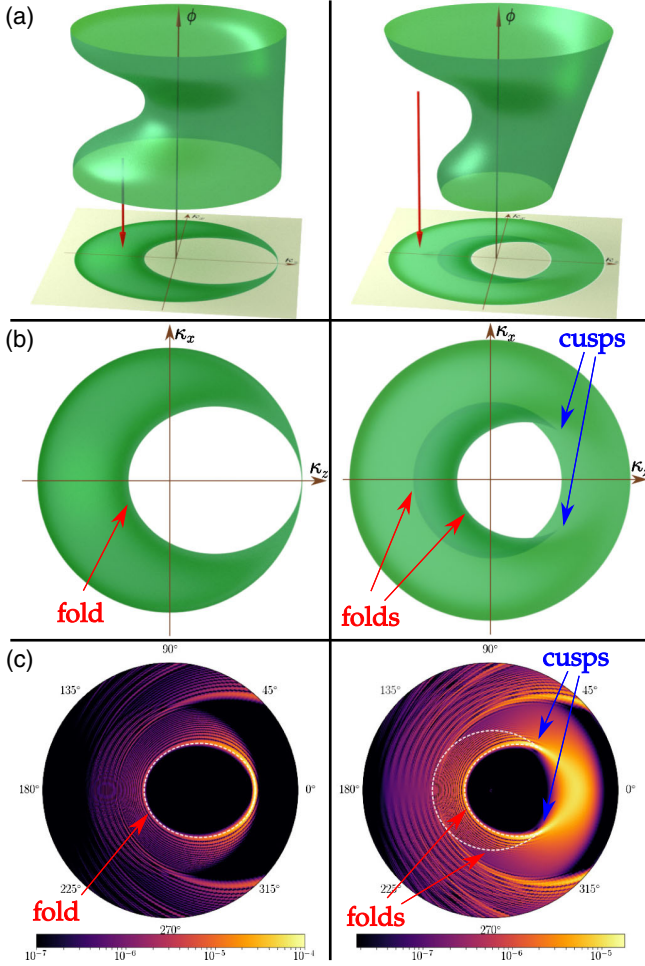
FIG. 1. The ray surfaces [stationary phase condition (4)] (a), their projections on the (κ_x, κ_z) plane (b), and corresponding numerically calculated spectra (c) in the electron frame: the radial coordinate is frequency, the angle is θ, and the color is the emission probability. The laser pulse is circularly polarized with envelope $|\mathbf{a}| = a_0 \cos^2(\pi\phi/\tau)$, $a_0 = 2.1$, and $\tau = 100\pi/\omega_{L,0}$, propagating to the right. Left column: unchirped pulse. Right column: chirped pulse with $\beta = 0.75$.

For the quasimonochromatic pulse the frequency is constant, $\omega_L(\phi) = \text{const}$, and the only type of caustic arising in the scattered spectrum is the fold caustic (Fig. 1, left column). The condition for the fold singularity on the ray surface is $d\mathbf{a}^2/d\phi = [\mathbf{a}^2]' = 0$. That is, a fold corresponds to an extremum in the pulse envelope, and to the peak in the scattered spectrum [26]. For a simple laser pulse with a single maximum in the envelope [38], the peak position is a function of the scattering angle θ given by

$$\omega_f(\theta) = \frac{n\omega_L}{1 + (1 - \cos\theta)(\frac{a_0^2}{4} + \frac{n\omega_L}{m})}, \qquad (5)$$

where $a_0^2 = \max_\phi \mathbf{a}^2$. In the vicinity of $\omega_f(\theta)$, the spectrum has the form of Airy functions and we see agreement with
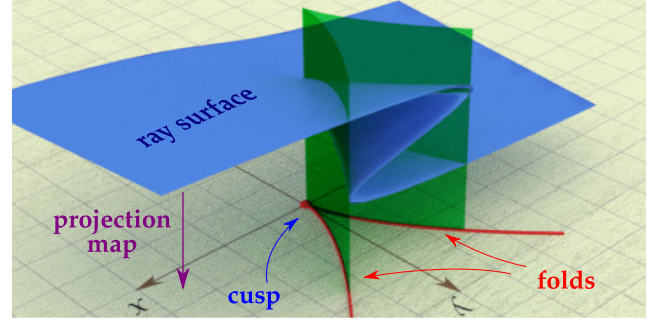
FIG. 2. Artistic image of a generic cusp as the singularity of a two-dimensional map. The projection of the surface to the (x, y) plane yields two folds (projected on red lines) coinciding and terminating in the cusp point.

the well-known theoretical predictions on the interference structure of the scattered radiation caused by two stationary points [14,26,39].

Let us now turn to the case of a linearly chirped pulse where we find not only folds to contribute to the spectrum, but also higher-dimensional cusps. For a linearly chirped laser pulse the instantaneous frequency varies with time according to $\omega_L(\phi) = \omega_{L,0} + \beta\phi/\tau$ with the linear chirp parameter β determining the rate of change of the frequency over the pulse duration τ. In this case, the locations of the singularities of the ray surface (4) are given by the conditions

$$\kappa^- \frac{[\mathbf{a}^2(\phi)]'}{4} = n\frac{\beta}{\tau}\left(1 - \frac{\kappa^-}{m}\right), \qquad (6)$$

$$[\mathbf{a}^2(\phi)]'' = 0, \qquad (7)$$

where Eq. (6) defines the loci of the folds for the chirped pulse and Eq. (7) determines their coincidence, defining the cusp singularity.

The typical situation with cusp-type singularities is illustrated in Fig. 1 (right column). For small values of chirp β there are two cusps for opposite values of κ_x, connected by two folds. For large values of β there are neither cusps nor folds. It can serve as the evidence of a higher-dimensional caustic taking place in between. In this situation we consider the chirp β as an additional control parameter, and the caustic consists in the coincidence of two cusps and their disappearance for increasing β. The space of control parameters is three dimensional now, and the described process is referred to as a "lips event" in the catastrophe theory [23,40], or as the celebrated "Zel'dovich pancake" [41] in astrophysics. The coincidence of the cusps happens in backscattering, $\theta = \pi$, due to the axial symmetry of the exponential in Eq. (3), making the lips event interesting for Compton sources.

From the physical point of view the cusps will result in a relatively bright narrow spot in the scattered spectrum at the cusp angle θ_c (Fig. 1, right column),
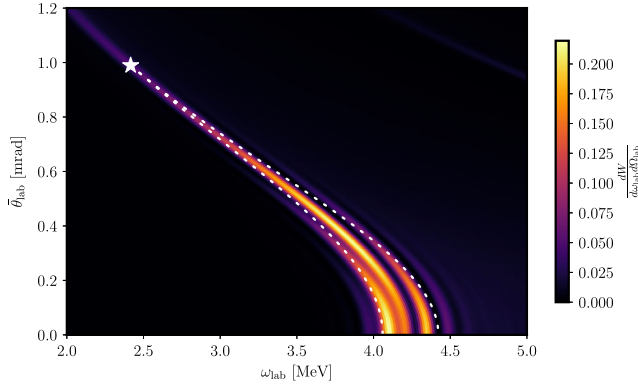
FIG. 3. Frequency-angle differential emission probability in the lab frame. The initial Lorentz factor of the electron is $\gamma = 1000$; the pulse shape is $|\mathbf{a}| = a_0 / \cosh(\phi/\tau)$; $\tau = 40\pi/\omega_{L,0}$, $a_0 = 1$, and the chirp parameter $\beta = 0.15$; $\bar{\theta}_{\text{lab}} := \pi - \theta_{\text{lab}}$. The on-axis radiation is Doppler up-shifted from $\omega_{L,0} = 1.55$ to ≈ 4 MeV, and strongly enhanced. The emitted radiation is effectively confined to the region bounded by the two folds and the cusp. Pushing the cusp closer to the axis by increasing β will constrain the radiation to a narrow bandwidth and well collimated beam of gamma rays.

$$\cos\theta_c = 1 - \frac{4\beta}{(\mathbf{a}^2)'\omega_L\tau - \mathbf{a}^2\beta}, \qquad (8)$$

where $\mathbf{a}$ and ω_L are evaluated at the point defined by Eq. (7). For $\theta_c < \theta \leq \pi$ one sees the interference between the three parts of the pulse, i.e., three stationary points, constrained by two folds. For $\theta \simeq \theta_c$ one observes a narrow peak in the scattered spectrum on top of a weaker pedestal. Beyond θ_c, closer to forward scattering, the width of the peak increases while only a single stationary point contributes. Equation (8) shows that the locations of the cusps can be controlled by the chirp parameter β, and, for a Compton source, the cusp angle should be close to the backscattering direction $\theta_c \to \pi$ for narrow-band and collimated emission. To see that, let us now go back to the lab frame.

When going to the lab frame the components of the photon momentum transform as $\kappa_{\perp,\text{lab}} = \kappa_\perp$ and $\kappa^-_{\text{lab}} = 2\gamma\kappa^-$, causing the ellipses in Fig. 1 to expand (contract) in the $-z$ $(+z)$ direction and the scattering angles θ to narrow towards the backscattering direction. The Jacobian of the Lorentz transformation $J = 1/[\gamma(1 + \beta\cos\theta_{\text{lab}})]$ strongly enhances the on-axis backscattered radiation close to $\theta_{\text{lab}} = \pi$ (and suppresses forward scattering), causing the strongest emission to be not exactly at the cusp position where emission is very narrow band (star marker), but for angles $\theta_{\text{lab}} > \theta_{c,\text{lab}}$. As one can clearly see in Fig. 3 this forces the emitted radiation to be strongly confined to the caustic region bounded by the two folds and the cusp. With increasing chirp β, the cusp is pushed towards the beam axis, pinching the folds and turning the emitted radiation into a collimated beam with enhanced spectral intensity and narrow bandwidth.
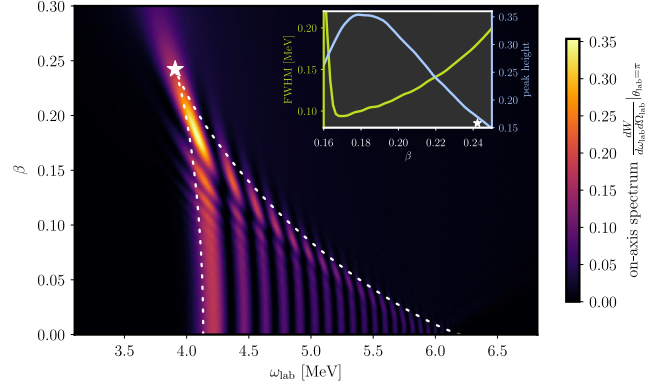
FIG. 4. The on-axis photon emission probability in the lab frame as a function of photon frequency and chirp parameter β shows the two folds (dashed curves) terminating in a cusp (star). In the vicinity of the cusp we see the typical Pearcey-integral pattern [23]. The spectrum (horizontal lineout) turns into a single narrow-band peak for a relatively large range of β values in the vicinity of the cusp (see inset). The pulse shape is $|\mathbf{a}| = a_0 / \cosh(\phi/\tau)$ with $\tau = 40\pi/\omega_{L,0}$ and $a_0 = 1$.

Figure 4 shows the on-axis emission probability as a function of different values of the chirp β (vertical axis), with the lips event; i.e., the coincidence of the cusp singularities on axis is depicted with a star at $\beta_c = 0.24$ [32]. The pinching of the two folds with increasing $\beta < \beta_c$ evokes a bright on-axis emission peak with a minimal bandwidth of 2.5% (FWHM) and the peak height more than doubled as compared to the unchirped case. The optimal chirp for this is $\beta_{\text{peak}} = 0.18$ for $a_0 = 1$, which can be determined by analyzing the Pearcey diffraction pattern in the vicinity of the cusps [32]. The required values of β can be realized with a relative laser bandwidth of 0.18 and a second order spectral phase (group delay dispersion) of $\varphi'' \approx 40$ fs^2, which can be achieved with today's laser technology [42]. Note that the developed approach is not constrained to the linear chirp only. Higher order chirping can be incorporated by additional control parameters, which can provide a higher degree of degeneracy of the stationary phase points, and a stronger radiation enhancement. It also provides new types of catastrophes, leaving the caustic analysis simple, but making the direct numerical parameter surveys very demanding [32].

In conclusion, in this Letter we applied the theory of the singularities of differentiable projection maps and caustics to analyze nonlinear Compton scattering spectra for short pulses with a variable pulse shape and chirp. The caustics are related to patterns in the nonlinear Compton spectra, which greatly simplifies the qualitative analysis of the spectra, and the inverse problem of tailoring laser pulses for the optimized narrow-band spectra.

We predict cusp singularities in the scattered spectrum for linearly chirped laser pulses and show that the location of the cusps can be tuned by the value of the linear chirp. The emitted radiation is effectively confined to the region

formed by the cusp and fold caustics. When the cusps are pushed close to the beam axis by tuning the chirp, the emitted radiation is pinched between two folds evoking bright narrow-band and collimated emission of gamma rays. The spectral caustics investigated in this Letter also provide a different view on the optimal chirping schemes for spectral bandwidth reduction [13–15,32].

The stability of caustics makes the provided analysis insensitive to the small variations of pulse properties, and electron beam effects, which is important for practical applications. This new perspective on the nonlinear Compton spectra can serve as a tool to design and optimize upcoming x-ray and gamma-ray Compton backscattering sources, guiding and complementing full-scale numeric simulations. Moreover, the method applied in this Letter can be also used for other processes of strong-field QED like nonlinear Breit-Wheeler pair production.

---

[*]v.kharin@gsi.de

[†]d.seipt@lancaster.ac.uk

[‡]s.rykovanov@gsi.de

[1] E. Esarey, S. K. Ride, and P. Sprangle, Phys. Rev. E **48**, 3003 (1993).

[2] H. Toyokawa, H. Ohgaki, T. Mikado, and K. Yamada, Rev. Sci. Instrum. **73**, 3358 (2002).

[3] G. Sarri, D. Corvan, W. Schumaker, J. Cole, A. Di Piazza, H. Ahmed, C. Harvey, C. H. Keitel, K. Krushelnick, S. Mangles *et al.*, Phys. Rev. Lett. **113**, 224801 (2014).

[4] D. Corvan, M. Zepf, and G. Sarri, Nucl. Instrum. Methods Phys. Res., Sect. A **829**, 291 (2016).

[5] V. Karagodsky and L. Schächter, Plasma Phys. Controlled Fusion **53**, 014007 (2011).

[6] V. G. Nedorezov, A. A. Turinge, and Y. M. Shatunov, Phys. Usp. **47**, 341 (2004).

[7] K. Khrennikov, J. Wenz, A. Buck, J. Xu, M. Heigoldt, L. Veisz, and S. Karsch, Phys. Rev. Lett. **114**, 195003 (2015).

[8] S. Chen, N. Powers, I. Ghebregziabher, C. Maharjan, C. Liu, G. Golovin, S. Banerjee, J. Zhang, N. Cunningham, A. Moorti *et al.*, Phys. Rev. Lett. **110**, 155003 (2013).

[9] S. G. Rykovanov, C. G. R. Geddes, J.-L. Vay, C. B. Schroeder, E. Esarey, and W. P. Leemans, J. Phys. B **47**, 234013 (2014).

[10] V. Y. Kharin, D. Seipt, and S. G. Rykovanov, Phys. Rev. A **93**, 063801 (2016).

[11] F. V. Hartemann, A. L. Troha, N. C. Luhmann Jr., and Z. Toffano, Phys. Rev. E **54**, 2956 (1996).

[12] I. Ghebregziabher, B. A. Shadwick, and D. Umstadter, Phys. Rev. ST Accel. Beams **16**, 030705 (2013).

[13] S. G. Rykovanov, C. G. R. Geddes, C. B. Schroeder, E. Esarey, and W. P. Leemans, Phys. Rev. Accel. Beams **19**, 030701 (2016).

[14] D. Seipt, S. G. Rykovanov, A. Surzhykov, and S. Fritzsche, Phys. Rev. A **91**, 033402 (2015).

[15] B. Terzić, K. Deitrick, A. S. Hofler, and G. A. Krafft, Phys. Rev. Lett. **112**, 074801 (2014).

[16] F. V. Hartemann and S. S. Q. Wu, Phys. Rev. Lett. **111**, 044801 (2013).

[17] D. Seipt, V. Kharin, S. Rykovanov, A. Surzhykov, and S. Fritzsche, J. Plasma Phys. **82**, 655820203 (2016).

[18] K. Krajewska, M. Twardy, and J. Z. Kamiński, Phys. Rev. A **89**, 052123 (2014).

[19] J. F. Nye, *Natural Focusing and Fine Structure of Light: Caustics and Wave Dislocations* (Institute of Physics Publishing, Bristol, 1999), p. 328.

[20] O. Raz, O. Pedatzur, B. D. Bruner, and N. Dudovich, Nat. Photonics **6**, 170 (2012).

[21] D. Seipt, A. Surzhykov, S. Fritzsche, and B. Kämpfer, New J. Phys. **18**, 023044 (2016).

[22] M. V. Berry and C. Upstill, Prog. Opt. **18**, 257 (1980).

[23] J. Nye, J. Opt. A: Pure Appl. Opt. **11**, 065708 (2009).

[24] A. I. Nikishov and V. I. Ritus, Sov. Phys. J. Exp. Theor. Phys. **19**, 529 (1964).

[25] A. I. Nikishov and V. I. Ritus, Sov. Phys. J. Exp. Theor. Phys. **19**, 1191 (1964).

[26] N. B. Narozhnyi and M. S. Fofanov, J. Exp. Theor. Phys. **83**, 14 (1996).

[27] M. Boca and V. Florescu, Phys. Rev. A **80**, 053403 (2009).

[28] D. Seipt and B. Kämpfer, Phys. Rev. A **83**, 022101 (2011).

[29] F. Mackenroth and A. Di Piazza, Phys. Rev. A **83**, 032106 (2011).

[30] K. Krajewska and J. Z. Kamiński, Phys. Rev. A **85**, 062102 (2012).

[31] D. M. Volkov, Z. Phys. **94**, 250 (1935).

[32] See Supplemental Material at http://link.aps.org/supplemental/10.1103/PhysRevLett.120.044802 for the details, which includes Refs. [33,34].

[33] S. Dali, The Swallow's Tail—Series on Catastrophes, Dali Theatre and Museum, Figueres, 1983.

[34] H. Korsch, A. Klumpp, and D. Witthaut, J. Phys. A **39**, 14947 (2006).

[35] M. Yeung, B. Dromey, S. Cousens, T. Dzelzainis, D. Kiefer, J. Schreiber, J. Bin, W. Ma, C. Kreuzer, J. Meyer-ter Vehn *et al.*, Phys. Rev. Lett. **112**, 123902 (2014).

[36] R. Thom, *Structural Stability and Morphogenesis* (Addison Wesley Publishing Company, Reading, MA, 1989).

[37] M. Berry, J. Phys. A **8**, 566 (1975).

[38] It is essential for the pulse to have an extremum in the corresponding point, not necessarily a maximum. But in that case the prefactors $B_{\varepsilon\sigma\sigma'}^n$ can be small and suppress the contribution of the caustic to the spectrum.

[39] D. Seipt and B. Kämpfer, Laser Phys. **23**, 075301 (2013).

[40] V. I. Arnol'd, *Catastrophe Theory* (Springer Science & Business Media, New York, 2003).

[41] V. Arnold, S. Shandarin, and Y. B. Zeldovich, Geophys. Astrophys. Fluid Dyn. **20**, 111 (1982).

[42] Z. Major, S. A. S. Trushin, I. Ahmad, M. Siebold, C. Wandt, S. Klingebiel, T.-j. Wang, J. A. Fülöp, A. Henig, S. Kruber, R. Weingartner, A. Popp, J. Osterhoff, R. Hörlein, J. Hein, V. Pervak, A. Apolonski, F. Krausz, and S. Karsch, Review of Laser Engineering **37**, 431 (2009).